

Communication

Phase Stability and Mechanical Properties Analysis of AlCo_xCrFeNi HEAs Based on First Principles

Fu Liang^{1,2}, Jin Du^{1,2,*}, Guosheng Su^{1,2}, Chonghai Xu^{1,2} , Chongyan Zhang³ and Xiangmin Kong³

¹ School of Mechanical Engineering, Qilu University of Technology (Shandong Academy of Sciences), Jinan 250300, China

² Shandong Institute of Mechanical Design and Research, Jinan 250300, China

³ Shandong Sanzuan Cemented Carbide Co., Ltd., Jinan 250300, China

* Correspondence: dj84105@qlu.edu.cn

Abstract: With the in-depth research on high-entropy alloys (HEAs), most of the current research uses experimental methods to verify the effects of the main elements of HEAs on the mechanical properties of the alloys. However, this is limited by the long experimental period and the influence of many external factors. The computer simulation method can not only effectively save costs and shorten the test cycle, but also help to discover new materials and broaden the field of materials. Therefore, in this paper, the physical properties (such as lattice constant, density and elastic constant) of AlCo_xCrFeNi (x = 0, 0.25, 0.5, 0.75, 1) HEAs were calculated based on the first-principles calculation method and virtual crystal approximate modeling method. It is found that AlCo_xCrFeNi HEAs have the best hardness and toughness properties, with a Co content of 0.5~0.7. The research results can provide theoretical guidance for the preparation of HEAs with optimal mechanical properties.

Keywords: high-entropy alloys; first principles; crystal structure; elastic properties; simulation and modeling



Citation: Liang, F.; Du, J.; Su, G.; Xu, C.; Zhang, C.; Kong, X. Phase Stability and Mechanical Properties Analysis of AlCo_xCrFeNi HEAs Based on First Principles. *Metals* **2022**, *12*, 1860. <https://doi.org/10.3390/met12111860>

Academic Editors: Sha Liu and Changming Fang

Received: 22 September 2022

Accepted: 27 October 2022

Published: 31 October 2022

Publisher's Note: MDPI stays neutral with regard to jurisdictional claims in published maps and institutional affiliations.



Copyright: © 2022 by the authors. Licensee MDPI, Basel, Switzerland. This article is an open access article distributed under the terms and conditions of the Creative Commons Attribution (CC BY) license (<https://creativecommons.org/licenses/by/4.0/>).

1. Introduction

High-entropy alloys (HEAs) are one of the hotspots in materials research in recent years [1]. They have excellent properties, such as high temperature resistance, corrosion resistance and radiation resistance [2,3], and broad application prospects in the fields of tools, molds and turbine blades [4–6]. As one of the most common types of HEAs, the AlCoCrFeNi HEA not only has excellent mechanical properties at room temperature, but also has little performance degradation in high-temperature environments. It is currently used in many fields such as cemented carbide and coated tools [7,8]. The current study found that the phase structure and microstructure of superalloys can be changed by adjusting the content of constituent elements [9,10]. This will in turn affect the mechanical properties of HEAs. On the one hand, the Co content affects the formation of the face-centered cubic (FCC) phase in the AlCo_xCrFeNi HEA. When the Co content is 0, Fe and Cr in HEAs can only generate disordered body-centered cubic (BCC) phase and it is difficult to generate stable FCC phase [11]. This in turn affects mechanical properties such as hardness and strength of the alloy. Therefore, an appropriate amount of Co content can significantly improve the mechanical properties of AlCo_xCrFeNi HEAs. On the other hand, since Co is a scarce resource in nature, it is widely used in metallurgy, the military industry, and the battery and catalysis industries. Therefore, saving Co has become an inevitable resource problem. However, the phase structure and mechanical properties of AlCoCrFeNi HEAs are mainly discussed from the aspects of material composition and preparation technology [12,13]. This experimental verification method has high cost and a long cycle. Using the first-principles calculation method, the ground state properties of the material system can be obtained by solving the Schrödinger equation through density functional theory [14–16]. Using this method can not only save costs, but also effectively shorten the test cycle. It

greatly increases the discovery speed of new materials and broadens the research scope of existing materials.

In conclusion, the first-principles method was used to analyze the effect of Co content on the phase structure and mechanical properties of $\text{AlCo}_x\text{CrFeNi}$ ($x = 0, 0.25, 0.5, 0.75, 1$) HEAs. The virtual crystal approximation method used in this paper can ensure the calculation accuracy and improve the calculation efficiency. It not only fills the gap in the research field of HEAs, but also has important guiding significance for practical production and application.

2. Materials and Methods

In this study, Cambridge sequential total energy package (CASTEP) module in Materials Studio software was adopted, which was developed by Cambridge University in England based on first principles [17]. In Figure 1, the $\text{AlCo}_x\text{CrFeNi}$ HEA models (FCC, BCC and HCP phase) were established by the virtual crystal approximation (VCA) method, and the AlCoCrFeNi HEA model (FCC phase) was established by the special quasi-random structures (SQS) method. The VCA method can effectively avoid the virtual atom or accumulated error caused by long-range structure in the modeling process. The exchange correlation functional adopted the Perdew–Burke–Ernzerhoff (PBE) functional in the generalized gradient approximation (GGA) [18]. The VCA models were calculated by ultrasoft pseudopotential, while the SQS model was calculated by norm-conserving pseudopotential [19–21]. The calculated parameters were obtained by convergence test in the process of geometric optimization. The convergence parameters were set as follows: the total energy tolerance is 10^{-5} eV/atom, the force tolerance is 0.03 eV/Å, the maximum stress is 0.05 GPa, and the maximum displacement is 0.001 Å. The cutoff energy of VCA is 630 eV, and that of the SQS model is 540 eV. The values of k points in Brillouin interval are $9 \times 9 \times 9$ and $6 \times 3 \times 3$, and the density parameter is 0.04 1/Å. The initial spin value in spin polarization is 5. After geometric optimization, the calculated lattice constant of the VCA model of the AlCoCrFeNi HEA (FCC phase) is 3.541 Å, while that of the SQS model is 3.54 Å. However, the calculated values are not much different from the lattice constant (3.591 Å) of the AlCoCrFeNi HEA prepared by Y. Garip by the RS method [22]. It can be proved that it is reliable to use the VCA method to study the $\text{AlCo}_x\text{CrFeNi}$ HEA. Therefore, the calculation parameters in this paper are set reasonably.

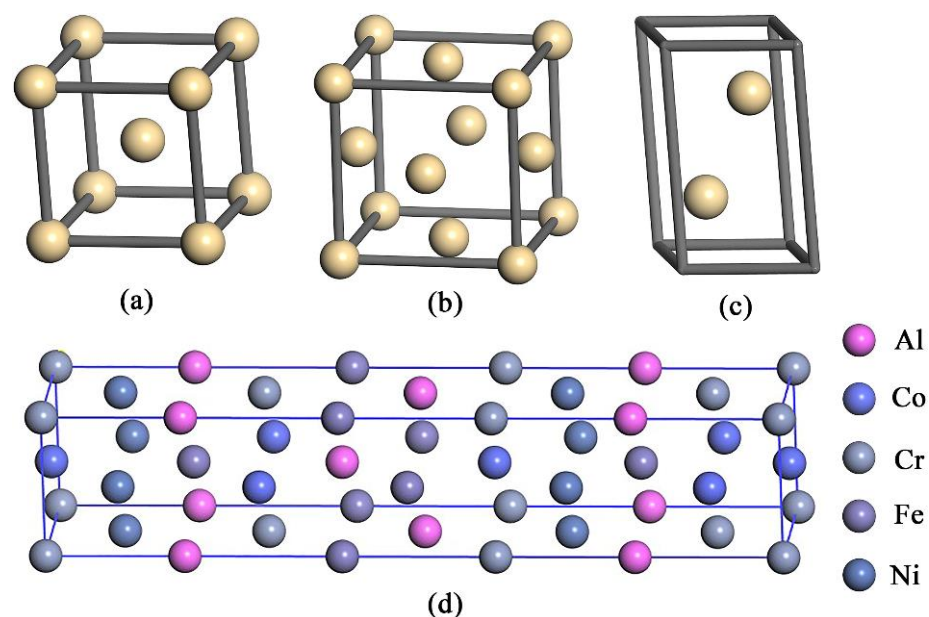


Figure 1. The $\text{AlCo}_x\text{CrFeNi}$ HEAs model constructed by VCA: (a) BCC phase, (b) FCC phase and (c) HCP phase. The model of AlCoCrFeNi HEA constructed by SQS: (d) FCC phase.

3. Results

3.1. Phase Stability

At present, in addition to the traditional XRD pattern to judge the alloy phase structure, the $\text{AlCo}_x\text{CrFeNi}$ ($x = 0, 0.25, 0.5, 0.75, 1$) HEAs can also be judged according to the empirical formula including mixed entropy ΔS_{mix} , mixed enthalpy ΔH_{mix} , valence electron concentration VEC , atomic radius difference δ , electronegativity difference $\Delta\chi$ and parameter Ω . Based on the obtained empirical parameters, it can provide guidance for the composition design and performance optimization of high-entropy alloys. Thus, blind design of high-entropy alloys is avoided, and the waste of experimental materials is reduced to a certain extent.

The mixed entropy ΔS_{mix} , mixed enthalpy ΔH_{mix} , valence electron concentration VEC , atomic radius difference δ , electronegativity difference $\Delta\chi$ and parameter Ω are calculated as follows [23–27]:

$$\Delta S_{\text{mix}} = -R \sum_{i=1, i \neq j}^n c_i \ln c_i \quad (1)$$

$$\Delta H_{\text{mix}} = \sum_{i=1, i \neq j}^n 4 \Delta H_{ij}^{\text{mix}} c_i c_j \quad (2)$$

$$VEC = \sum_{i=1}^n c_i (VEC)_i \quad (3)$$

$$\delta = \sqrt{\sum_{i=1}^n c_i (1 - r_i/\bar{r})^2}, \bar{r} = \sum_{i=1}^n c_i r_i \quad (4)$$

$$\Delta\chi = \sqrt{\sum_{i=1}^n c_i (\chi_i - \bar{\chi})^2}, \bar{\chi} = \sum_{i=1}^n c_i \chi_i \quad (5)$$

$$\Omega = \frac{T_m \Delta S_{\text{mix}}}{|\Delta H_{\text{mix}}|}, T_m = \sum_{i=1}^n c_i (T_m)_i \quad (6)$$

where R is the molar gas constant, C_i and $(VEC)_i$ are the atomic ratio and the number of valence electrons of the i -th component, \bar{r} is the average atomic radius of the HEAs, c_i and r_i are the atomic ratio and atomic radius of the i -th component, $\bar{\chi}$ is the average Pauling electronegativity of HEA, c_i and χ_i are the atomic ratio and Pauling electronegativity of the i -th component, and $(T_m)_i$ is the melting temperature of the i -th component.

The structure rules of alloy phase were predicted by VEC : $VEC < 6.87$ is the BCC phase; $6.87 < VEC < 8$ is the BCC+FCC phase; $VEC > 8$ is the FCC phase. From Table 1, $VEC > 6.87$ indicates that the addition of Co will promote the formation of FCC phase in $\text{AlCo}_x\text{CrFeNi}$ HEAs [23]. Usually, $\delta \leq 6.6\%$ is considered to form a stable solid solution structure. From Table 1, $\delta \leq 6.6\%$ indicates that $\text{AlCo}_x\text{CrFeNi}$ HEAs can form a stable solid solution structure and the degree of alloy lattice distortion is gradually reduced [24]. Electronegativity is defined as the ability of an atom to gain or lose electrons [25]. The greater the electronegativity of the element, the stronger the ability of the element to gain and lose electrons, and the stronger its non-metallic properties. Conversely, elements have strong ductility and metallic properties [26]. From Table 1, the small change in $\Delta\chi$ indicates that the ductilities of the HEAs are not very different. Parameter Ω is obtained by thermodynamic calculation of mixing entropy, mixing enthalpy and melting point. When $\Omega > 1$, it can be used to judge the phase stability in the alloy [27]. From Table 1, it is found that the phase structure of the alloy will gradually become stable with the increase in Co content.

Table 1. The mixed entropy ΔS_{mix} , mixed enthalpy ΔH_{mix} , valence electron concentration VEC , atomic radius difference δ , electronegativity difference $\Delta\chi$, melting point T_m and parameter Ω of $AlCo_xCrFeNi$ ($x = 0, 0.25, 0.5, 0.75, 1$) HEA.

Alloys	ΔS_{mix} /[J/(K · mol)]	ΔH_{mix} /(kJ/mol)	VEC	δ /%	$\Delta\chi$	T_m /K	Ω
AlCrFeNi	11.56	−13.24	6.75	6.27	0.122	1035.60	0.90
AlCo _{0.25} CrFeNi	12.72	−13.07	6.88	6.14	0.119	1046.55	1.02
AlCo _{0.5} CrFeNi	13.14	−12.84	7.00	6.01	0.122	1056.31	1.08
AlCo _{0.75} CrFeNi	13.30	−12.59	7.11	5.89	0.121	1065.03	1.12
AlCoCrFeNi	13.39	−12.32	7.20	5.78	0.121	1072.85	1.17

In addition, the relative stability of phases in HEAs can be judged by thermodynamics. The CASTEP module is used to calculate the crystal energy of $AlCo_xCrFeNi$ HEA models with different phase structures (FCC, BCC and HCP phase). The stability of the crystal phase structure can be judged by the energy level. In Table 2, when HEA is in the FCC phase, the crystal energy is the lowest. This shows that the FCC phase is easier to form and exists more stably in $AlCo_xCrFeNi$ HEAs than the BCC phase and HCP phase. This also proves the rationality of using the FCC phase to study the mechanical properties of $AlCo_xCrFeNi$ HEAs in this paper.

Table 2. The crystal energies of different phase structures (BCC, FCC and HCP phases) of $AlCo_xCrFeNi$ ($x = 0, 0.25, 0.5, 0.75, 1$) HEAs were modeled by VCA method.

Alloys	Energy/eV		
	BCC	FCC	HCP
AlCrFeNi	−2229.51	−2229.54	−2229.53
AlCo _{0.25} CrFeNi	−2259.47	−2259.54	−22593.52
AlCo _{0.5} CrFeNi	−2272.61	−2272.67	−2272.64
AlCo _{0.75} CrFeNi	−2276.52	−2276.6	−2276.57
AlCoCrFeNi	−2275.32	−2275.38	−2275.34

3.2. Mechanical Properties

Lattice constant is the basic structural parameter of crystal material, which is used to describe the change in atomic space position caused by the change in composition or stress of a crystal material. It not only reflects the interaction between atoms, but also has a certain relationship with the density of the material. CASTEP can calculate the corresponding stress by inputting the strain. The elastic constant is finally obtained by linear fitting of the stress–strain relationship [28,29]. The addition of Co will cause the FCC phase to appear in the $AlCo_xCrFeNi$ ($x = 0, 0.5, 1, 1.5, 2$) HEAs, and the FCC phase is also an important factor determining the strength of the alloy. Therefore, an $AlCo_xCrFeNi$ ($x = 0, 0.25, 0.5, 0.75, 1$) HEA was constructed by the VCA method based on the unit cell (FCC phase). Since the VCA method introduces the concept of mixing in the level of pseudopotential, each atom in the unit cell has the proportion of multiple atoms at the same time. After the geometry optimization, the overall model of the high-entropy alloy has little change, and its lattice constant and density are shown in Table 3. From Table 3, with the increase in Co content, the lattice constant of HEAs gradually decreased and the density increased gradually. The calculated density is not much different from the theoretical density calculated by addition (error < 4 %). This shows that the lattice distortion of $AlCo_xCrFeNi$ ($x = 0, 0.5, 1, 1.5, 2$) HEAs gradually decreases when Co is added, which is also the same as the δ calculation result.

Table 3. Lattice constant and density of AlCo_xCrFeNi (x = 0, 0.25, 0.5, 0.75, 1) HEAs.

Alloys	Lattice Parameter/Å	Mass Density/(g/cm ³)	Theoretical Density/(g/cm ³)
AlCrFeNi	3.556	6.74	6.6
AlCo _{0.25} CrFeNi	3.55	7.07	6.79
AlCo _{0.5} CrFeNi	3.541	7.09	6.9
AlCo _{0.75} CrFeNi	3.538	7.12	7.01
AlCoCrFeNi	3.537	7.14	7.1

The size of the material's elastic constants (C_{11} , C_{12} , C_{44}) determines the bulk modulus K , shear modulus G , Young's modulus E and Poisson's ratio ν , which play important roles in determining the mechanical properties of the material. The effect of Co on the mechanical properties of AlCo_xCrFeNi HEAs was further studied. The paper calculated the elastic constants (C_{11} , C_{12} , C_{13}), polycrystalline elastic moduli (K , G , E , ν), anisotropy index A_{VR} and hardness H_v of AlCo_xCrFeNi HEAs. The calculation formula is shown below [30,31], and the calculation results are listed in Table 4.

$$K = \frac{C_{11} + 2C_{12}}{3} \quad (7)$$

$$G_V = \frac{1}{5} (3C_{44} + C_{11} - C_{12}) \quad (8)$$

$$G_R = \frac{5(C_{11} - C_{12})C_{44}}{4C_{44} + 3(C_{11} - C_{12})} \quad (9)$$

$$G = \frac{G_V + G_R}{2} \quad (10)$$

$$E = \frac{9KG}{3K + G} \quad (11)$$

$$\nu = \frac{3K - 2G}{2(3K + G)} \quad (12)$$

$$A_{VR} = \frac{C_{11} - C_{12} - 2C_{44}}{C_{11} - C_{44}} \quad (13)$$

$$H_v = 2 \times \left(\frac{G^3}{B^2} \right)^{0.585} - 3 \quad (14)$$

where C_{ij} is the elastic constant and G_V and G_R are the elastic moduli G obtained by the Voigt and Reuss methods.

Table 4. Calculated elastic constant, elastic modulus, ν and A_{VR} of AlCo_xCrFeNi (x = 0, 0.25, 0.5, 0.75, 1) HEA.

Alloys	C_{11} /GPa	C_{12} /GPa	C_{44} /GPa	$C_{11}-C_{44}$ /GPa	K /GPa	G /GPa	E /GPa	K/G /GPa	ν	A_{VR}
AlCrFeNi	172	97	91	82	122	64	162	1.91	0.29	2.41
AlCo _{0.25} CrFeNi	182	97	78	104	125	61	157	2.05	0.28	1.85
AlCo _{0.5} CrFeNi	180	99	89	90	126	65	166	1.94	0.32	2.21
AlCo _{0.75} CrFeNi	185	113	74	111	137	56	147	2.45	0.32	2.05
AlCoCrFeNi	188	115	79	110	139	59	153	2.36	0.32	2.14

In Table 4, Cauchy pressure is positive ($C_{12} - C_{44} > 0$) [32], indicating that the HEA is a ductile material. To facilitate the comparison of mechanical properties, the elastic constants and polycrystalline elastic moduli of AlCo_xCrFeNi (x = 0, 0.25, 0.5, 0.75, 1) HEAs are plotted in Figure 2. It is generally believed that K reflects the bonding strength between atoms, molecules and ions in the material. On the macroscopic scale, K represents

the incompressibility of the material. The larger the bulk modulus K of the material, the stronger its incompressibility and the worse its ductility. The shear modulus G represents the ability of the material to resist shear deformation. The larger the shear modulus G , the better the rigidity of the material and the worse the ductility. Young's modulus E is a standard used to measure the resistance of materials to deformation. The larger the value, the greater the stress required for the material to elastically deform, that is, the less likely the material is to deform. A material with $A_{VR} = 0$ is generally considered to be elastically isotropic, otherwise it is elastically anisotropic. It can be seen from Figure 2 that the bulk modulus (K) increases with the increase in Co content, while the shear modulus (G) does not change significantly [33]. The Young's modulus is the largest when the Co content is 0.5, and the material has the best resistance to deformation. This shows that $\text{AlCo}_{0.5}\text{CrFeNi}$ HEA has the strongest resistance to deformation and better ductility. $A_{VR} > 0$ indicates [34] that HEAs are elastic anisotropic materials.

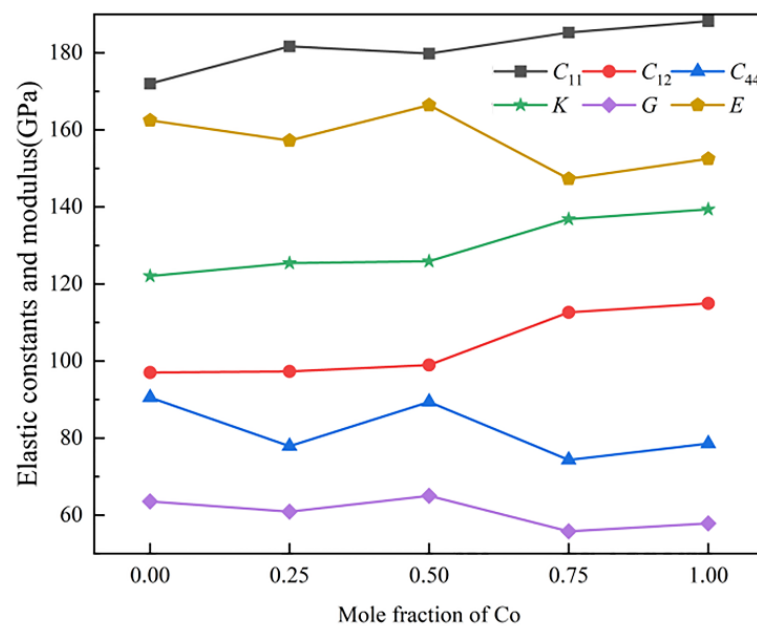


Figure 2. The elastic constants (C_{11} , C_{12} , C_{44}) and modulus (K , G , E) of $\text{AlCo}_x\text{CrFeNi}$ ($x = 0, 0.25, 0.5, 0.75, 1$) HEAs.

The ductility or brittleness of alloy materials can be judged by the Poisson's ratio ν and the ratio of bulk modulus to shear modulus K/G [35]. Materials with a Poisson's ratio ν of about $1/3$ are considered ductile materials, while materials in other ranges are called brittle materials and the maximum value cannot exceed 0.5. When the ratio of bulk modulus to shear modulus is greater than 1.75, the material is a ductile material, otherwise it is a brittle material. In Figure 3, the Poisson's ratio ν of $\text{AlCo}_x\text{CrFeNi}$ ($x = 0, 0.25, 0.5, 0.75, 1$) HEAs is about $1/3$ and belongs to ductile materials. $K/G > 1.75$ indicates that the toughness of the material is gradually enhanced with the addition of Co, and the toughness of $\text{AlCo}_{0.75}\text{CrFeNi}$ is the best.

In Figure 4, the calculated microhardnesses of $\text{AlCo}_x\text{CrFeNi}$ HEAs are 774 Hv, 663 Hv, 777 Hv, 444 Hv and 477 Hv. The experimental microhardnesses of the high-entropy alloy prepared by Faruk Kaya [36] by the suction-cast method are 500 Hv, 575 Hv, 530 Hv, 480 Hv and 520 Hv. The experimental microhardnesses of the high-entropy alloy prepared by the SHS method are 440 Hv, 425 Hv, 510 Hv, 380 Hv and 425 Hv. The microhardness of the alloy is different with different preparation methods. However, HEAs prepared by the suction-cast method have a finer microstructure. They will have higher hardness than HEAs prepared by the self-propagating-high-temperature synthesis (SHS) method. With the increase in Co content, the BCC phase in $\text{AlCo}_x\text{CrFeNi}$ HEA is gradually transformed into FCC phase. Finally, the BCC+FCC dual-phase structure is formed in the alloy. The

analysis results show that with the increase in Co content, the calculated values of hardness are the same as the experimental values obtained by the SHS method. When the content of Co is low, there is a big error between the calculated results and the experimental values. This is due to the low FCC phase content in HEAs. When the Co content increases, the calculated hardness is between the two experimental values. This is because part of the BCC phase in HEAs is converted into the FCC phase. This also proves that the calculation is in line with the reality.

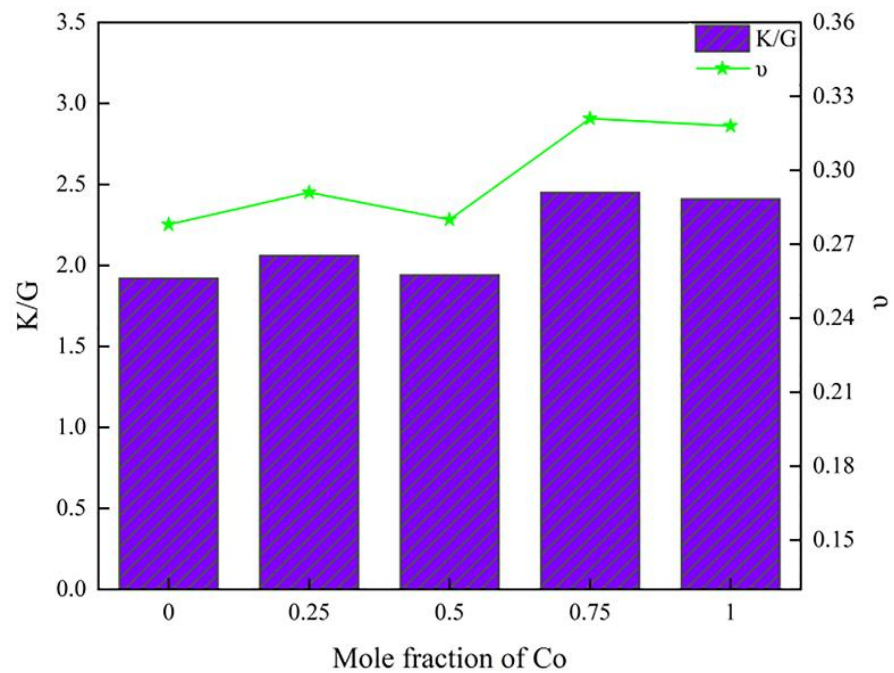


Figure 3. The calculated K/G and v of AlCo_xCrFeNi (x = 0, 0.25, 0.5, 0.75, 1) HEAs.

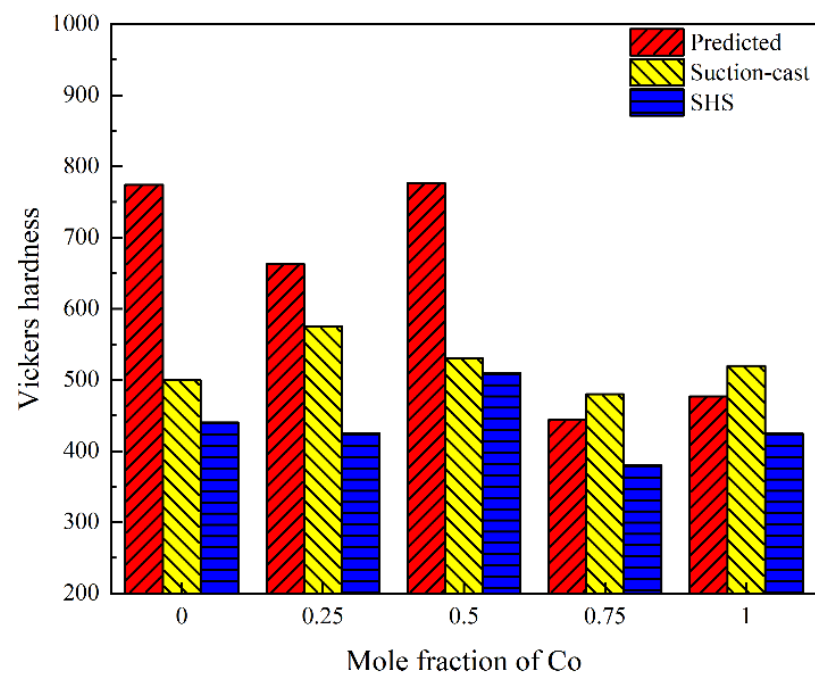


Figure 4. The predicted and experimental hardness of AlCo_xCrFeNi (x= 0, 0.25, 0.5, 0.75, 1) HEAs.

4. Conclusions

In this paper, the $\text{AlCo}_x\text{CrFeNi}$ ($x = 0, 0.25, 0.5, 0.75, 1$) HEAs were calculated based on the first-principles-based density functional method, and it is found that the $\text{AlCo}_x\text{CrFeNi}$ HEAs can form a stable solid solution structure. The addition of Co affects the formation of the FCC phase in HEAs, resulting in the decrease in density and the increase in lattice constant. It also plays an important role in improving the mechanical properties of HEAs. The research shows that the $\text{AlCo}_{0.5}\text{CrFeNi}$ HEA has the highest hardness, while the $\text{AlCo}_{0.75}\text{CrFeNi}$ HEA has the best toughness. Therefore, the optimal balance point of Co content in $\text{AlCo}_x\text{CrFeNi}$ HEAs may be between 0.5 and 0.75, which also provides some guidance for specific experiments.

Author Contributions: F.L.: conceptualization, methodology, software, investigation, writing—original draft preparation. J.D.: conceptualization, methodology, investigation, supervision, writing—review and editing. G.S.: supervision, formal analysis. C.X.: supervision, validation. C.Z.: supervision. X.K.: resources. All authors have read and agreed to the published version of the manuscript.

Funding: This work was supported by the Natural Science Foundation of China (52275438,51675289), The Natural Science Foundation of Shandong Province (ZR2020ME160) and the Basic research project of pilot project of integration of science, education and production (Qi-lu University of Technology (Shandong Academy of Sciences)) (2022PY007).

Institutional Review Board Statement: Not applicable.

Informed Consent Statement: Not applicable.

Data Availability Statement: The data are not publicly available due to privacy.

Conflicts of Interest: The authors declare no conflict of interest.

References

1. Ke, B.R.; Sun, Y.C.; Zhang, Y.; Wang, W.R.; Wang, W.M.; Ma, P.Y.; Ji, W.; Fu, Z.Y. Powder metallurgy of high-entropy alloys and related composites: A short review. *Int. J. Miner. Metall. Mater.* **2021**, *28*, 931–943. [[CrossRef](#)]
2. Asadikiya, M.; Yang, S.; Zhang, Y.; Lemay, C.; Apelian, D.; Zhong, Y. A review of the design of high-entropy aluminum alloys: A pathway for novel Al alloys. *J. Mater. Sci.* **2021**, *56*, 12093–12110. [[CrossRef](#)]
3. Vaidya, M.; Muralikrishna, G.M.; Murty, B.S. High-entropy alloys by mechanical alloying: A review. *J. Mater. Res.* **2019**, *34*, 664–686. [[CrossRef](#)]
4. Wan, Y.; Mo, J.; Wang, X.; Zhang, Z.; Shen, B.; Liang, X. Mechanical Properties and Phase Stability of WTaMoNbTi Refractory High-Entropy Alloy at Elevated Temperatures. *Acta Metall. Sin. (Engl. Lett.)* **2021**, *34*, 1585–1590. [[CrossRef](#)]
5. Xu, J.; Peng, S.; Li, Z.Y.; Jiang, S.Y.; Xie, Z.H.; Paul, M.; Lu, H. Remarkable cavitation erosion–corrosion resistance of CoCrFeNiTiMo high-entropy alloy coatings. *Corros. Sci.* **2021**, *190*, 109663. [[CrossRef](#)]
6. Pickering, E.J.; Carruthers, A.W.; Barron, P.J.; Middleburgh, S.C.; Armstrong, D.E.J.; Gandy, A.S. High-Entropy Alloys for Advanced Nuclear Applications. *Entropy* **2021**, *23*, 98. [[CrossRef](#)]
7. Wei, L.; Liu, X.; Gao, Y.; Peng, X.; Hu, N.; Chen, M. Phase, microstructure and mechanical properties evaluation of AlCoCrFeNi high-entropy alloy during mechanical ball milling. *Intermetallics* **2021**, *138*, 107310. [[CrossRef](#)]
8. Wang, J.J.; Kou, Z.D.; Fu, S.; Wu, S.S.; Liu, S.N.; Yan, M.Y.; Ren, Z.Q.; Wang, D.; You, Z.H.; Lan, S.; et al. Ultrahard BCC-AlCoCrFeNi bulk nanocrystalline high-entropy alloy formed by nanoscale diffusion-induced phase transition. *J. Mater. Sci. Technol.* **2022**, *115*, 29–39. [[CrossRef](#)]
9. Li, H.J.; Zhao, L.; Yang, Y.; Zong, H.X.; Ding, X.D. Improving radiation-tolerance of bcc multi-principal element alloys by tailoring compositional heterogeneities. *J. Nucl. Mater.* **2021**, *555*, 153140. [[CrossRef](#)]
10. Yeh, J.W.; Lin, S.J.; Chin, T.S.; Gan, J.Y.; Chen, S.K.; Shun, T.T.; Tsau, C.H.; Chou, S.Y. Formation of simple crystal structures in Cu-Co-Ni-Cr-Al-Fe-Ti-V alloys with multiprincipal metallic elements. *Metall. Mater. Trans. A* **2004**, *35*, 2533–2536. [[CrossRef](#)]
11. Kang, M.J.; Lim, K.R.; Won, J.W.; Na, Y.S. Effect of Co content on the mechanical properties of A2 and B2 phases in $\text{AlCo}_x\text{CrFeNi}$ high-entropy alloys. *J. Alloys Compd.* **2018**, *769*, 808–812. [[CrossRef](#)]
12. Strumza, E.; Hayun, S. Comprehensive study of phase transitions in equiatomic AlCoCrFeNi high-entropy alloy. *J. Alloys Compd.* **2021**, *856*, 158220. [[CrossRef](#)]
13. Karlsson, D.; Beran, P.; Riekehr, L.; Tseng, J.C.; Harlin, P.; Jansson, U.; Cedervall, J. Structure and phase transformations in gas atomized AlCoCrFeNi high entropy alloy powders. *J. Alloys Compd.* **2022**, *893*, 162060. [[CrossRef](#)]
14. Nong, Z.S.; Zhu, J.C.; Yu, H.L.; Lai, Z.H. First principles calculation of intermetallic compounds in FeTiCoNiVCrMnCuAl system high entropy alloy. *Trans. Nonferrous Met. Soc. China.* **2012**, *22*, 1437–1444. [[CrossRef](#)]

15. Tong, Y.; Bai, L.; Liang, X.; Hua, M.; Liu, J.; Li, Y.; Zhang, J.; Hu, Y. Mechanical performance of (NbTaW)_{1-x}Mox (x = 0, 0.05, 0.15, 0.25) refractory high entropy alloys: Perspective from experiments and first principles calculations. *J. Alloys Compd.* **2021**, *873*, 159740. [[CrossRef](#)]
16. Chen, Y.; Zhao, Q.; Wu, H.; Fang, Q.; Li, J. Effect of interstitial N atom on physical and mechanical properties of FeCoCrNiMn high-entropy alloys: A first-principles study. *Phys. B* **2021**, *615*, 413078. [[CrossRef](#)]
17. Segall, M.D.; Lindan, P.J.D.; Probert, M.J.; Pickard, C.J.; Hasnip, P.J.; Clark, S.J.; Payne, M.C. First-principles simulation: Ideas, illustrations and the CASTEP code. *Journal of Physics. Condens. Matter.* **2002**, *14*, 0953–8984. [[CrossRef](#)]
18. Mayahi, R. An investigation concerning generalized stacking fault behavior of AlCoxCrFeNi (0.25 ≤ x ≤ 2) high entropy alloys: Insights from first-principles study. *J. Alloys Compd.* **2020**, *818*, 152928. [[CrossRef](#)]
19. Perdew, J.P.; Burke, K.; Ernzerhof, M. Generalized Gradient Approximation Made Simple. *Phys. Rev. Lett.* **1996**, *77*, 3865–3868. [[CrossRef](#)]
20. Hamann, D.R. Generalized norm-conserving pseudopotentials. *Phys. Rev. B* **1989**, *40*, 2980–2987. [[CrossRef](#)]
21. Rogal, Ł.; Szklarz, Z.; Bobrowski, P.; Kalita, D.; Garzeł, G.; Tarasek, A.; Kot, M.; Szlezzynger, M. Microstructure and Mechanical Properties of Al–Co–Cr–Fe–Ni Base High Entropy Alloys Obtained Using Powder Metallurgy. *Met. Mater. Int.* **2019**, *25*, 930–945. [[CrossRef](#)]
22. Saeid, A.; Parisa, E.; Masayoshi, F.; Kaveh, E. High-entropy ceramics: Review of principles, production and applications. *Mater. Sci. Eng. R.* **2021**, *146*, 100644. [[CrossRef](#)]
23. Chen, L.; Xuanhong, H.; Yueyi, W.; Xiaowei, Z.; Hongxi, L. First-principles calculation of the effect of Ti content on the structure and properties of TiVNbMo refractory high-entropy alloy. *Mater. Res. Express.* **2020**, *7*, 106516. [[CrossRef](#)]
24. Mole, S.J.; Zhou, X.F.; Liu, R.F. Density Functional Theory (DFT) Study of Enthalpy of Formation. 1. Consistency of DFT Energies and Atom Equivalents for Converting DFT Energies into Enthalpies of Formation. *J. Phys. Chem. C* **1996**, *100*, 14665–14671. [[CrossRef](#)]
25. Gan, G.Y.; Ma, L.; Luo, D.M.; Jiang, S.; Tang, B.Y. Influence of Al substitution for Sc on thermodynamic properties of HCP high entropy alloy Hf_{0.25}Ti_{0.25}Zr_{0.25}Sc_{0.25-x}Al_x from first-principles investigation. *Phys. B* **2020**, *593*, 412272. [[CrossRef](#)]
26. Yang, X.; Zhang, Y. Prediction of high-entropy stabilized solid-solution in multi-component alloys. *Mater. Chem. Phys.* **2012**, *132*, 233–238. [[CrossRef](#)]
27. Liu, S.Y.; Zhang, S.; Liu, S.; Li, D.J.; Li, Y.; Wang, S. Phase stability, mechanical properties and melting points of high-entropy quaternary metal carbides from first-principles. *J. Eur. Ceram. Soc.* **2021**, *41*, 6267–6274. [[CrossRef](#)]
28. Clark, S.J.; Segall, M.D.; Pickard, C.J.; Hasnip, P.J.; Probert, M.I.J.; Refson, K.; Payne, M.C. First principles methods using CASTEP. *Z. Krist. Cryst. Mater.* **2005**, *220*, 567–570. [[CrossRef](#)]
29. Shang, S.; Wang, Y.; Liu, Z.-K. First-principles elastic constants of alpha- and theta-Al₂O₃. *Appl. Phys. Lett.* **2007**, *90*, 101909. [[CrossRef](#)]
30. Liu, S.Y.; Liu, C.; Zhang, S.; Liu, S.; Li, D.J.; Li, Y.; Wang, S. Phase diagram and mechanical properties of fifteen quaternary high-entropy metal diborides: First-principles calculations and thermodynamics. *J. Appl. Phys.* **2022**, *131*, 075105. [[CrossRef](#)]
31. Liu, S.Y.; Zhang, S.; Liu, S.; Li, D.J.; Niu, Z.; Li, Y.; Wang, S. Stability and mechanical properties of single-phase quinary high-entropy metal carbides: First-principles theory and thermodynamics. *J. Eur. Ceram. Soc.* **2022**, *42*, 3089–3098. [[CrossRef](#)]
32. Tong, Y.; Bai, L.; Liang, X.; Chen, Y.; Zhang, Z.; Liu, J.; Li, Y.; Hu, Y. Influence of alloying elements on mechanical and electronic properties of NbMoTaWX (X = Cr, Zr, V, Hf and Re) refractory high entropy alloys. *Intermetallics* **2020**, *126*, 106928. [[CrossRef](#)]
33. Li, X. Third-order elastic constants and anharmonic properties of three fcc high-entropy alloys from first-principles. *J. Alloys Compd.* **2018**, *764*, 906–912. [[CrossRef](#)]
34. Yao, X.J.; Shi, X.F.; Wang, Y.P.; Gan, G.Y.; Tang, B.Y. The mechanical properties of high entropy (-like) alloy Wx(TaTiVCr)_{1-x} via first-principles calculations. *Fusion Eng. Des.* **2018**, *137*, 35–42. [[CrossRef](#)]
35. Hu, Y.L.; Bai, L.H.; Tong, Y.G.; Deng, D.Y.; Liang, X.B.; Zhang, J.; Li, Y.J.; Chen, Y.X. First-principle calculation investigation of NbMoTaW based refractory high entropy alloys. *J. Alloys Compd.* **2020**, *827*, 153963. [[CrossRef](#)]
36. Kaya, F.; Yetiş, M.; Selimoğlu, G.İ.; Derin, B. Influence of Co content on microstructure and hardness of AlCoxCrFeNi (0 ≤ x ≤ 1) high-entropy alloys produced by self-propagating high-temperature synthesis. *Eng. Sci. Technol.* **2022**, *27*, 101003. [[CrossRef](#)]